Title: Anti-pronator components are essential to effectively alter lower-limb kinematics and kinetics in individuals with flexible flatfoot

Authors: Gauthier Desmyttere[a,*], Maryam Hajizadeh[b], Jacinte Bleau[b], Sébastien Leteneur[d], Mickael Begon[a,c]

Affiliations:

[a] École de Kinésiologie et des Sciences de l'Activité Physique, Université de Montréal, Campus Laval, 1700 rue Jacques Tétreault, Laval, QC, Canada H7N 0B6

[b] Institut de Génie Biomédical, Université de Montréal, Campus Laval, 1700 rue Jacques Tétreault, Laval, QC, Canada H7N 0B6

[c] Laboratoire Orthopédique Médicus, 2520 Boul. St-Joseph, Montréal, QC, Canada H1Y 2A2

[d] Université Polytechnique Hauts-de-France, UMR 8201 - LAMIH - Laboratoire d'Automatique de Mécanique et d'Informatique Industrielles et Humaines, F-59313 Valenciennes, France

Corresponding author:

Gauthier Desmyttere

Postal address: 1700 rue Jacques Tétreault, Laval, QC, Canada H7N 0B6

Email address: gauthier.desmyttere@umontreal.ca

Word count:

Abstract: 239 words.

Main text: 3450 words.

Abstract

Background: Foot orthoses are commonly used to correct for foot alterations and especially address excessive foot pronation in individuals with flatfeet. In recent years, 3D printing has taken a key place in orthotic manufacturing processes as it offers more options and can be patient specific. Hence, the purpose of this study was to evaluate whether stiffness of 3D printed foot orthoses and a newly designed rearfoot posting have an effect on lower limb kinematics and kinetics in individuals with flatfeet.

Methods: Nineteen patients with flexible flatfeet were provided two pairs of customized 3D printed ¾ length orthotics. Foot orthoses were of different stiffness and could feature a rearfoot posting, consisting of 2-mm carbon fiber plate. Lower limb kinematics and kinetics were computed using a multi-segment foot model. One-way ANOVAs using statistical non-parametric mapping, refined by effect sizes, were performed to determine the magnitude of the effect between conditions.

Findings: Foot orthoses stiffness had little effect on midfoot and forefoot biomechanics. Reductions in midfoot eversion and forefoot abduction were observed during short periods of stance with rigid foot orthoses. Adding the posting had notable effects on rearfoot kinematics and on the ankle and knee kinetics in the frontal plane; it significantly reduced the eversion angle and inversion moment at the ankle, and increased the knee abduction moment.

Interpretation: Using an anti-pronator component is more effective than increasing foot orthoses stiffness to observe a beneficial impact of foot orthoses on the control of excessive foot pronation in individuals with flatfeet.

Keywords: Flatfoot; Foot orthoses; Gait analysis; Multi-segment foot model

1. Introduction

Flatfoot is a common deformity referring to an abnormally low medial longitudinal arch and which has been reported to affect around 20-25% of the adult population (Dunn et al., 2004; Pita-Fernandez et al., 2017). Flatfoot can be classified into rigid or flexible, the latter being more prevalent and characterized by a partial or total collapse of the medial longitudinal arch upon weight-bearing (Shibuya et al., 2010). This condition usually induces several biomechanical changes, in proportion to the severity of deformity (Shin et al., 2019), interfering with normal foot function. Thus, individuals with flatfeet have been associated with a greater eversion, plantarflexion and internal rotation of the rearfoot, as well as a more abducted forefoot (Hösl et al., 2014; Levinger et al., 2010). Furthermore, these kinematics changes contribute to a higher ankle inversion moment (Hunt and Smith, 2004). Although not all flatfeet are symptomatic, there is a higher incidence of individuals with foot pain and an increased risk of injury, which could negatively affect their quality of life (Pita-Fernandez et al., 2017; Riskowski et al., 2013).

Foot orthoses (FOs) have commonly been used as a conservative treatment to correct for foot alterations, alleviate eventual pains and prevent injuries in individuals with flatfeet (Banwell et al., 2015). Further, Cheung et al. (2011) found that custom-made FOs were more effective than prefabricated ones to control excessive foot pronation, However, due to the variety of FOs geometrical designs, materials and protocols that have been used to investigate their effect, there is still low evidence of their beneficial effect in flatfeet (Banwell et al., 2014; Desmyttere et al., 2018). To better understand the effect of FOs, and especially the influence of their geometrical design on lower limb kinematics and kinetics in individuals with flatfeet, the review conducted by Desmyttere et al. (2018) highlighted that FOs including a medial posting represent the most effective intervention to reduce rearfoot eversion and therefore control excessive foot pronation in flatfeet. Regarding joint moments, medially posted FOs were shown to decrease the ankle inversion moment and may therefore alleviate lower-limb disorders related to flatfeet (Peng et al., 2020; Telfer et al., 2013). Moreover, when incrementally changing a rearfoot posting level (2°), a dose-response effect at the rearfoot and knee joint has been reported (Telfer et al., 2013), highlighting the need for an accurate and patient-specific FOs construction. However, to our knowledge, all studies investigating FOs effect on joint moments in individuals with flatfeet were conducted using a simplified representation of foot as a single segment, while recent literature showed the benefits of intrinsic foot joints kinetic analyses (Deschamps et al., 2017; Saraswat et al., 2014). The use of multi-segment kinetic foot models, recently developed (Bruening et al., 2012; Deschamps et al., 2017), might therefore bring valuable information on how FOs act on foot function.

In recent years, the advent of 3D printing as a manufacturing process in orthotics has made it possible to address various needs. Indeed, 3D printing may allow for a reduction of cost and labor time for podiatrists, and is a repeatable and accurate manufacturing process that enables to reach the desired degree of customization for each patient (Davia-Aracil et al., 2018; Shahar et al., 2020). In addition, the use of 3D printing techniques in orthotics offer a wide range of possibilities in terms of material and design, and thus have facilitated the production of innovative custom shapes and geometries in comparison to traditional fabrication techniques. In a recent study, Desmyttere et al. (2020) showed that 3D printed FOs, and their effect on foot kinematics of healthy people, can be modulated by changing their stiffness using different geometries of honeycombs but also by inserting newly designed anti-pronator components under the heel. Yet, to our knowledge, no study has investigated the effect of customized FOs material properties, such as stiffness, on kinematics and kinetics in a flatfeet population.

Therefore, the aim of this study was to evaluate if an increase in stiffness of 3D printed FOs and/or the addition of an innovative anti-pronator component are associated to beneficial biomechanical changes in individuals with flexible flatfeet during gait. Further, the use of a kinetic multi-segment foot model will help provide a better understanding of underlying mechanisms.

2. Methods

2.1. Participants

Potential participants were recruited by experienced podiatrists. To be eligible for inclusion, participants had to have a pronated foot type as defined by the Foot Posture Index (Redmond et al., 2006), an arch height flexibility >16 mm/kN (Zifchock et al., 2017), report pain, have no history of wearing FOs prior to this study, as well as no lower limb surgery or injury during the last three months. Plus, they had to present normal lower-limb range of motions and no leg length discrepancy (<0.5 cm) (Surgeons, 1965). Nineteen patients participated in this study (13 females and 6 males, age: 37.6 ± 14.0 years, height: 166.7 ± 9.9 cm, body mass: 68.9 ± 11.5 kg, FPI: 7.8 ± 1.3; AHF: 25.6 ± 7.3 mm/kN; shoe size in the range 36-44 EU). All participants gave their written informed consent prior to data collection. All testing procedures were approved by the institution ethics committee (17-145-CERES-D).

2.2. Foot orthoses

FOs used in this study were customized based on a 3D scan of participants foot shapes, obtained in semi-weight bearing using foot impression boxes while the feet were maintained in a neutral subtalar position. They were ¾ length, designed using a CAD software (Shapeshift3D, Montreal, CA), and 3D printed in Nylon 12 by selective laser sintering. They consisted of a plate of 1.5 mm thickness superimposed to honeycombs (Fig. 1). Two pairs of different stiffnesses, named flexible and rigid for the purpose of this study, were fabricated by changing the height of the honeycomb cells. This process was automated through the CAD software according to participant's body weight and arch height flexibility. The average height of honeycomb cells at the medial arch region was 2.0 mm for flexible FOs and 3.2 mm for rigid FOs. The posting used in the present study consisted of a 2 mm carbon fiber plate that can be added under the orthotic heel (Fig. 1B-C). Neutral with an extension under the medial arch, the posting was inspired by a Thomas heel shoe modification {Zamosky, 1964 #47} and mainly designed to stabilize and control the FO and foot, especially at rearfoot and under the medial arch throughout the stance phase. Experiments were performed using a standardized running shoe model (860 v8, New Balance, USA). Four conditions were investigated: (i) shoe only, referred as control, (ii) flexible FOs, (iii) flexible FOs with posting, referred as posting, (iv) rigid FOs.

2.3. Experimental procedure

Participants had a 2-weeks period of accommodation, in a randomized order, to each of their FOs (flexible and the rigid). Approximately 1-month later, participants came to the laboratory for the main evaluation. Prior to data collection, participants were given 5-min of walking practice on a treadmill at a comfortable speed for acclimation and to establish the speed for the following measurements. In addition, a static trial and hip and knee functional movements were acquired to personalize a multibody kinematic model. Then, each participant walked for 3-min at his predetermined speed under each condition. A 5-min rest period between conditions was given to avoid any fatigue effects. Participants were blinded to the FOs conditions. Conditions were randomized, except for the posting condition that was always the last condition due to the need to glue it on the FO's heel.

2.4. Data collection

An 18-camera motion analysis system (VICON, Oxford, UK) sampling at 100 Hz and an instrumented split-belt treadmill (Bertec, Columbus, USA) sampling at 2000 Hz were used to collect kinematic and kinetic data. A set of 30 reflective markers was placed on the participants' pelvis and right lower limb to model the pelvis, the thigh, the shank and the foot as multi-segment (Supplementary Material). On the foot, reflective wand mounted markers were placed according to the Rizzoli foot model to track the rearfoot, midfoot and forefoot motion (Leardini et al., 2007). Circular holes (⌀ 2.5 cm) were made in the standardized shoes to put reflective markers directly on the foot skin. To ensure accurate foot marker reapplication each time FOs were changed, pen marks were made on the skin. Data were synchronized and recorded during the last 30-s of each 3-min trial to ensure participants were familiarized with each condition.

2.5. Data processing

All data analyses were performed using Matlab software (R2018a, The Mathworks, Natick, USA). Marker trajectories and ground reaction forces (GRF) were low-pass filtered using a fourth-order, zero lag, Butterworth filter with cutoff frequencies of 6 and 10 Hz, respectively.
A 6-segment, 21-degree-of freedom (DoF) kinematic model was personalized and defined with ball-and-socket joints using the static trial and the functional movements (Pelvis [6 DoF], Thigh [3 DoF], Shank [3 DoF], Rearfoot [3 DoF], Midfoot [3 DoF], Forefoot [3 DoF]). Hip joint center of rotation was estimated using the SCoRE algorithm (Ehrig et al., 2006), whereas knee joint

center of rotation was estimated using the SARA algorithm (Ehrig et al., 2007). Bony landmarks were used to define other joint centers of rotation. The shank-rearfoot (hereafter referred as ankle joint) center was defined as the midpoint between malleoli, the rearfoot-midfoot (hereafter referred as Chopard joint) center was defined as the midpoint between the cuboid and the navicular, and the midfoot-forefoot (hereafter referred as Lisfranc joint) center was defined as the base of the second metatarsal bone. Generalized coordinates were computed using an extended Kalman filter algorithm in Biorbd (Michaud and Begon, 2021). In addition to 3D joint rotations, the medial longitudinal arch (MLA) angle, defined by the markers on the calcaneus, the navicular tuberosity, and the first metatarsal head, was calculated as the angle between the two three-dimensional vectors bounded by those markers (Caravaggi et al., 2019).

Joint kinetics were calculated in Biorbd using inverse dynamics based on generalized coordinates and GRF. Unusable data due to cross-over steps were removed prior to further analysis. Segment inertial properties were calculated from the anthropometric model of De Leva (1996). The mass of the foot was arbitrary divided by three and distributed over the rearfoot, midfoot and forefoot segments. At each frame, GRF was applied to one foot segment according to the anterior-posterior location of the center of pressure (Bruening and Takahashi, 2018). Joint moments were normalized to body mass (Nm/kg). Data were then normalized from 0 to 100% of the stance phase, based on gait events detected using a 20 N force threshold of the GRF vertical component. Chopart and Lisfranc joint moments were only considered after the center of pressure was anterior to their respective joint center (38% and 56% of stance on average respectively).

2.6. Statistical analysis

Curve analyses were conducted using one-dimensional Statistical non-Parametric Mapping (SnPM) code (www.spm1d.org) (Pataky et al., 2015). Non-parametric tests were used as the d'Agostino-Pearson K2 test revealed that the data were not normally distributed. SnPM one-way ANOVAs, with a significance level set at $\alpha=0.05$, were performed to test the effect of FOs stiffness and posting on lower limb kinematics and joint moments. SnPM post-hoc t-tests with Bonferroni correction (0.05/6=0.0083) were used for multiple comparisons. To determine the magnitude of significant differences, Cohen's d effect sizes were computed over the entire stance phase per *post-hoc* comparison. If statistical differences were found, only the time periods with a Cohen's d exceeding 0.4 (moderate), for at least 10% of the stance phase, were judged relevant and considered for further analysis (Armijo-Olivo et al., 2011). When it occurred, the beginning and end of these time periods, the mean difference (MD) throughout these periods, as well as the mean effect size (MES) were reported. We decided to account for time periods of at least 10% of the stance phase in order to conduct a more functional data analysis.

3. Results

Significant time periods found in kinematics and kinetics between conditions and their corresponding MD and MES are reported in Tables 1 and 2.

3.1. Kinematics

At the ankle joint (Fig. 2), both flexible and rigid FOs increased the rearfoot dorsiflexion compared to the control and posting conditions (clusters: ~10-65% of stance; MD=1.3° to 1.6°). Compared to the other three conditions, the posting induced a decrease in rearfoot eversion up to 2.0° throughout the stance. The rearfoot was also in a more abducted position during short periods when using the posting compared to the control condition (cluster 1: 16-33%, MD=1.3°; cluster 2: 76-86%, MD=0.9°).

At the Chopart joint (Fig. 2), midfoot dorsiflexion was increased by 1.1° on average using flexible FOs (cluster 1: 0-12%, cluster 2: 31-55%), posting (54-69%), and rigid FOs (0-66%) compared to the control condition. In contrast with the other conditions, and especially rigid FOs (0-83%; MD=1.1°), the posting increased midfoot eversion. Midfoot eversion was also increased for a short period during midstance using flexible FOs compared to rigid FOs (MD=0.7°). In the transverse plane, the posting condition induced a decrease in midfoot abduction of about 0.6° compared to flexible (84-93%) and rigid FOs (cluster 1: 22-40%, cluster 2: 76:97%).

At the Lisfranc joint (Fig. 2), an increase in forefoot plantarflexion of 1.0° on average was observed when using the flexible FOs in comparison with the control (cluster 1: 20-32%, cluster 2: 43-87%) and posting conditions (cluster 1: 22-31%, cluster 2: 61-79%). A similar increase was seen with the rigid FOs compared to the control condition (64-82%). In the frontal plane, flexible and rigid FOs increased forefoot eversion by 1.1° on average during early stance (clusters: ~0-20%) compared to the control condition, whereas the posting induced an increase of about 1° throughout the stance. The forefoot was also less abducted when using the rigid FOs compared to the flexible ones (58-74%, MD=-0.8°).

3.2. Joint moments

A reduction in the inversion moment at the ankle joint up to 0.029 Nm/kg was observed with the use of the posting compared to the other conditions (*vs.* control: 8-78%; *vs.* flexible: 10-37%; vs. rigid: 11-29%) (Fig. 3A). A decrease was also observed with the rigid FOs compared to the control condition (30-73%, MD=0.023 Nm/kg). In the transverse plane, and in comparison with the control and flexible FOs, the posting increased the abduction moment up to 0.030 Nm/kg at the ankle joint (clusters: ~65-100%) (Fig. 3B).

At Chopart and Lisfranc joint (Fig 3C-D), posting decreased the plantarflexion moment compared to the control condition (55-76%, MD=-0.074 Nm/kg and 57-71%, MD = -0.061 Nm/kg at Chopart and Lisfranc joint respectively).

At the knee joint (Fig. 4), the posting induced an increase in the abduction moment around the first and second peaks compared to the control condition (cluster 1: 24-34%, MD=0.047 Nm/kg; cluster 2: 59-77%, MD=0.035 Nm/kg), and around the second peak compared to flexible FOs (64-82%, MD=0.036).

4. Discussion

This study aimed to investigate the effect of customized 3D printed FOs stiffness, as well as the addition of an anti-pronator component, on lower limb kinematics and kinetics during walking in flexible flatfeet. Our findings suggest that there is little to no effect due to FOs stiffness on lower-limb kinematics and kinetics, and that the use of an anti-pronator component (*i.e.* the posting) is necessary to observe significant changes on foot kinematics, as well as foot and knee kinetics in individuals with flexible flatfeet.

Previous studies comparing individuals with flatfeet *versus* healthy participants have reported several foot kinematic and kinetic differences, namely an everted and plantarflexed position of the rearfoot, a greater internal rotation of the tibia, a more abducted position of the forefoot, and an increased ankle inversion moment (Hösl et al., 2014; Hunt and Smith, 2004; Levinger et al., 2010). Results from the present study showed that our customized 3D printed FOs altered mostly the foot kinematics since no significant effect on knee and hip kinematics was found. Flexible and rigid FOs altered mainly the foot sagittal plane kinematics since they reduced rearfoot plantarflexion and midfoot dorsiflexion, previously reported as being increased in individuals with flatfeet (Caravaggi et al., 2018). However, contrary to our previous study reporting significant effects on frontal and transverse plane foot kinematics when increasing the stiffness of 3D printed FOs (Desmyttere et al., 2020), very little effects were observed in the present study. These results may be explained by the variability introduced while customizing FOs, and therefore stiffnesses, for each participant, whereas in our previous study the same pairs of flexible and rigid 3D printed FOs were used for all healthy participants. Yet, the rigid FOs induced a decrease in ankle inversion moment compared to the control condition, which was not observed with the flexible FOs. Although no significant difference regarding ankle inversion moment was observed between the rigid and flexible FOs, increasing the stiffness may reduce the functional demand on invertor muscles such as the tibialis posterior and therefore possible overuse injuries (McClay and Baitch, 2003; Peng et al., 2020).

In line with a recent review highlighting the need for anti-pronator components such as medial posting to observe significant biomechanical changes reflecting a better control of the excessive pronation in individuals with flatfeet (Desmyttere et al., 2018), adding the posting to the flexible FOs had significant effects on frontal plane foot kinematics. Indeed, rearfoot eversion was significantly decreased, especially at early stance and midstance (>2°). As assumed by Genova and Gross (2000), using the posting might therefore be associated with clinical improvements. To compensate for the reduction in rearfoot eversion, and since rearfoot and midfoot frontal motion are strongly coupled (Takabayashi et al., 2018), an increase in midfoot eversion was observed when using the posting, and more specifically compared to the rigid FOs. Increasing locally the stiffness at medial arch may therefore help to better control midfoot frontal plane motion. In addition, the greater forefoot inversion that usually accompanied the increased rearfoot eversion in individuals with flatfeet was decreased in this study (Hösl et al., 2014). Therefore, our results suggest that frontal plane foot kinematics in individuals with flatfeet can also be controlled using neutral postings with an extension under the medial arch. Further, the posting induced a reduction in rearfoot adduction, another variable contributing to flatten the arch (Levinger et al., 2010). Yet, the extra depth (2 mm) under the heel brought while adding the posting cancelled the beneficial effects on the sagittal plane. Hence, the design of our posting could be improved to avoid the foot to be lifted inside the shoe but remains promising. Looking at joint moments, and as reported in previous studies (Peng et al., 2020; Telfer et al., 2013), the decrease in rearfoot eversion induced by the posting was associated with a significant decrease in ankle inversion moment, highlighting its beneficial effect on the ankle joint. In addition, we observed an increase in knee abduction moment due to the posting. This change might be explained by a coupling motion existing between the foot and the leg (Williams et al., 2001), and a more medial position of the GRF vector increasing the moment arm and therefore the abduction moment at the knee. As flatfeet may lead to patellofemoral pain syndrome, due to an excessive tibial and femoral internal rotation and lateral patellar displacement, FOs with posting could represent a beneficial intervention to improve pain and physical function by bringing the knee abduction moment toward normal values (Johnston and Gross, 2004). The same applies for individuals with posterior tibial tendon dysfunction in which knee abduction moment is lower than for asymptomatic population (Swart et al., 2012). However, caution should be paid while increasing knee abduction moment as it could have adverse effects and may lead to the development or the progression of medial compartment knee osteoarthritis (Miyazaki et al., 2002). Values in the present study are, however, still in the range of those reported for healthy subjects and not exceeding 0.65-0.70 Nm/kg, which would increase the probability of knee medial compartment problems (Schmalz et al., 2006). Hence, our results suggest that the addition of a flat posting could be effective to control excessive pronation and reduce the risk for individuals with flatfeet to sustain foot and knee pain associated with their foot posture.

Some limitations from this study should be considered. First, our multi-segment foot kinetic model uses a partitioning of GRF based on the position of the center of pressure which could lack of accuracy compared to a method partitioning the GRF based on the plantar pressure distribution (Bruening and Takahashi, 2018). Second, error could have been introduced in the computation of kinematics results due to the application of skin markers based on palpation and the presence of soft tissue artifacts (Schallig et al., 2021; Telfer et al., 2010). Hence, as the reported mean angle differences were relatively small (0.5 to 2.0°), a degree of precaution needs to be applied when interpreting the results from the present study. Third, some bias might have arisen due to the FOs order. Indeed, as the posting had to be glued on the flexible FOs, this condition was always the last one. Fourth, the posting condition was only tested on the flexible FOs, and the combination of the posting and the rigid FOs might have brought valuable information. Fifth, this study only reported the kinematic and kinetic effects of the orthotics after four weeks of use. The investigation of their long-term effects as well as their effect on muscle activations, plantar pressures or patients' quality of life could bring more insight and explain their potential therapeutic effectiveness. Finally, this study was conducted with a population of symptomatic flexible flatfeet, and it should be kept in mind that most flexible flatfeet are physiologic, asymptomatic, and require no treatment (Harris, 2010).

5. Conclusion

The addition of anti-pronator components on FOs seems more suitable than modifying FO stiffness to alter gait patterns in individuals with flatfeet. Indeed, postings can induce significant biomechanical changes in the frontal plane, such as a reduction in rearfoot eversion angle and ankle inversion moment, as well as an increase in knee abduction moment, highlighting its beneficial effect on the control of excessive foot pronation.

Acknowledgements: This work was supported by the TransMedTech institute and the NSERC R&D Coop with Medicus, Caboma and MedTech.

References

Armijo-Olivo, S., Warren, S., Fuentes, J., Magee, D.J., 2011. Clinical relevance vs. statistical significance: Using neck outcomes in patients with temporomandibular disorders as an example. Manual therapy 16, 563-572.

Banwell, H.A., Mackintosh, S., Thewlis, D., 2014. Foot orthoses for adults with flexible pes planus: a systematic review. Journal of foot and ankle research 7, 23.

Banwell, H.A., Thewlis, D., Mackintosh, S., 2015. Adults with flexible pes planus and the approach to the prescription of customised foot orthoses in clinical practice: a clinical records audit. The Foot 25, 101-109.

Bruening, D.A., Cooney, K.M., Buczek, F.L., 2012. Analysis of a kinetic multi-segment foot model part II: kinetics and clinical implications. Gait & posture 35, 535-540.

Bruening, D.A., Takahashi, K.Z., 2018. Partitioning ground reaction forces for multi-segment foot joint kinetics. Gait & posture 62, 111-116.

Caravaggi, P., Matias, A.B., Taddei, U.T., Ortolani, M., Leardini, A., Sacco, I.C., 2019. Reliability of medial-longitudinal-arch measures for skin-markers based kinematic analysis. Journal of biomechanics 88, 180-185.

Caravaggi, P., Sforza, C., Leardini, A., Portinaro, N., Panou, A., 2018. Effect of plano-valgus foot posture on midfoot kinematics during barefoot walking in an adolescent population. Journal of foot and ankle research 11, 55.

Cheung, R.T., Chung, R.C., Ng, G.Y., 2011. Efficacies of different external controls for excessive foot pronation: a meta-analysis. British journal of sports medicine 45, 743-751.

Davia-Aracil, M., Hinojo-Pérez, J.J., Jimeno-Morenilla, A., Mora-Mora, H., 2018. 3D printing of functional anatomical insoles. Computers in Industry 95, 38-53.

De Leva, P., 1996. Adjustments to Zatsiorsky-Seluyanov's segment inertia parameters. Journal of biomechanics 29, 1223-1230.

Deschamps, K., Eerdekens, M., Desmet, D., Matricali, G.A., Wuite, S., Staes, F., 2017. Estimation of foot joint kinetics in three and four segment foot models using an existing proportionality scheme: application in paediatric barefoot walking. Journal of Biomechanics 61, 168-175.

Desmyttere, G., Hajizadeh, M., Bleau, J., Begon, M., 2018. Effect of foot orthosis design on lower limb joint kinematics and kinetics during walking in flexible pes planovalgus: A systematic review and meta-analysis. Clinical Biomechanics 59, 117-129.

Desmyttere, G., Leteneur, S., Hajizadeh, M., Bleau, J., Begon, M., 2020. Effect of 3D printed foot orthoses stiffness and design on foot kinematics and plantar pressures in healthy people. Gait & Posture 81, 247-253.

Dunn, J., Link, C., Felson, D., Crincoli, M., Keysor, J., McKinlay, J., 2004. Prevalence of foot and ankle conditions in a multiethnic community sample of older adults. American journal of epidemiology 159, 491-498.

Ehrig, R.M., Taylor, W.R., Duda, G.N., Heller, M.O., 2006. A survey of formal methods for determining the centre of rotation of ball joints. Journal of biomechanics 39, 2798-2809.

Ehrig, R.M., Taylor, W.R., Duda, G.N., Heller, M.O., 2007. A survey of formal methods for determining functional joint axes. Journal of biomechanics 40, 2150-2157.

Genova, J.M., Gross, M.T., 2000. Effect of foot orthotics on calcaneal eversion during standing and treadmill walking for subjects with abnormal pronation. Journal of Orthopaedic & Sports Physical Therapy 30, 664-675.

Harris, E.J., 2010. The natural history and pathophysiology of flexible flatfoot. Clinics in podiatric medicine and surgery 27, 1-23.

Hösl, M., Böhm, H., Multerer, C., Döderlein, L., 2014. Does excessive flatfoot deformity affect function? A comparison between symptomatic and asymptomatic flatfeet using the Oxford Foot Model. Gait & posture 39, 23-28.

Hunt, A.E., Smith, R.M., 2004. Mechanics and control of the flat versus normal foot during the stance phase of walking. Clinical biomechanics 19, 391-397.

Johnston, L.B., Gross, M.T., 2004. Effects of foot orthoses on quality of life for individuals with patellofemoral pain syndrome. Journal of Orthopaedic & Sports Physical Therapy 34, 440-448.

Leardini, A., Benedetti, M.G., Berti, L., Bettinelli, D., Nativo, R., Giannini, S., 2007. Rear-foot, mid-foot and fore-foot motion during the stance phase of gait. Gait & posture 25, 453-462.

Levinger, P., Murley, G.S., Barton, C.J., Cotchett, M.P., McSweeney, S.R., Menz, H.B., 2010. A comparison of foot kinematics in people with normal-and flat-arched feet using the Oxford Foot Model. Gait & posture 32, 519-523.

McClay, I.D., Baitch, S., 2003. Effect of inverted orthoses on lower-extremity mechanics in runners. Medicine and science in sports and exercise 35, 2060-2068.

Michaud, B., Begon, M., 2021. biorbd: A C++, Python and MATLAB library to analyze and simulate the human body biomechanics. Journal of Open Source Software 6, 2562.

Miyazaki, T., Wada, M., Kawahara, H., Sato, M., Baba, H., Shimada, S., 2002. Dynamic load at baseline can predict radiographic disease progression in medial compartment knee osteoarthritis. Annals of the rheumatic diseases 61, 617-622.

Pataky, T.C., Vanrenterghem, J., Robinson, M.A., 2015. Zero-vs. one-dimensional, parametric vs. non-parametric, and confidence interval vs. hypothesis testing procedures in one-dimensional biomechanical trajectory analysis. Journal of biomechanics 48, 1277-1285.

Peng, Y., Wong, D.W.-C., Wang, Y., Chen, T.L.-W., Tan, Q., Chen, Z., Jin, Z., Zhang, M., 2020. Immediate Effects of Medially Posted Insoles on Lower Limb Joint Contact Forces in Adult Acquired Flatfoot: A Pilot Study. International Journal of Environmental Research and Public Health 17, 2226.

Pita-Fernandez, S., Gonzalez-Martin, C., Alonso-Tajes, F., Seoane-Pillado, T., Pertega-Diaz, S., Perez-Garcia, S., Seijo-Bestilleiro, R., Balboa-Barreiro, V., 2017. Flat foot in a random population and its impact on quality of life and functionality. Journal of clinical and diagnostic research: JCDR 11, LC22.

Redmond, A.C., Crosbie, J., Ouvrier, R.A., 2006. Development and validation of a novel rating system for scoring standing foot posture: the Foot Posture Index. Clinical biomechanics 21, 89-98.

Riskowski, J.L., Dufour, A.B., Hagedorn, T.J., Hillstrom, H.J., Casey, V.A., Hannan, M.T., 2013. Associations of foot posture and function to lower extremity pain: results from a population-based foot study. Arthritis care & research 65, 1804-1812.

Saraswat, P., MacWilliams, B.A., Davis, R.B., D'Astous, J.L., 2014. Kinematics and kinetics of normal and planovalgus feet during walking. Gait & posture 39, 339-345.

Schallig, W., Streekstra, G.J., Hulshof, C.M., Kleipool, R.P., Dobbe, J.G., Maas, M., Harlaar, J., van der Krogt, M.M., van den Noort, J.C., 2021. The influence of soft tissue artifacts on multi-segment foot kinematics. Journal of Biomechanics 120, 110359.

Schmalz, T., Blumentritt, S., Drewitz, H., Freslier, M., 2006. The influence of sole wedges on frontal plane knee kinetics, in isolation and in combination with representative rigid and semi-rigid ankle–foot-orthoses. Clinical Biomechanics 21, 631-639.

Shahar, F.S., Sultan, M.T.H., Shah, A.U.M., Safri, S.N.A., 2020. A Comparative Analysis between Conventional Manufacturing and Additive Manufacturing of Ankle-Foot Orthosis. Applied Science and Engineering Progress 13, 96-103.

Shibuya, N., Jupiter, D.C., Ciliberti, L.J., VanBuren, V., La Fontaine, J., 2010. Characteristics of adult flatfoot in the United States. The Journal of foot and ankle surgery 49, 363-368.

Shin, H.S., Lee, J.H., Kim, E.J., Kyung, M.G., Yoo, H.J., Lee, D.Y., 2019. Flatfoot deformity affected the kinematics of the foot and ankle in proportion to the severity of deformity. Gait & Posture 72, 123-128.

Surgeons, A.A.o.O., 1965. Joint motion: method of measuring and recording. Churchill Livingstone.

Swart, N.M., van Linschoten, R., Bierma-Zeinstra, S.M., van Middelkoop, M., 2012. The additional effect of orthotic devices on exercise therapy for patients with patellofemoral pain syndrome: a systematic review. British Journal of Sports Medicine 46, 570-577.
Takabayashi, T., Edama, M., Yokoyama, E., Kanaya, C., Inai, T., Tokunaga, Y., Kubo, M., 2018. Changes in kinematic coupling among the rearfoot, midfoot, and forefoot segments during running and walking. Journal of the American Podiatric Medical Association 108, 45-51.
Telfer, S., Abbott, M., Steultjens, M.P., Woodburn, J., 2013. Dose–response effects of customised foot orthoses on lower limb kinematics and kinetics in pronated foot type. Journal of biomechanics 46, 1489-1495.
Telfer, S., Morlan, G., Hyslop, E., Semple, R., Rafferty, D., Woodburn, J., 2010. A novel device for improving marker placement accuracy. Gait & posture 32, 536-539.
Williams, D.S., McClay, I.S., Hamill, J., Buchanan, T.S., 2001. Lower extremity kinematic and kinetic differences in runners with high and low arches. Journal of applied biomechanics 17, 153-163.
Zifchock, R.A., Theriot, C., Hillstrom, H.J., Song, J., Neary, M., 2017. The Relationship between arch height and arch flexibility: a proposed arch flexibility classification system for the description of multidimensional foot structure. Journal of the American Podiatric Medical Association 107, 119-123.

Figure captions

Fig. 1 - Medial view of a flexible FO without (A) and with (B) posting. Bottom view of a flexible FO with posting (C).

Fig. 2 - Foot kinematics during the stance phase. Top graph shows the mean kinematics of each condition with 95 % confidence interval cloud (control condition). In the bottom graph, bars indicate significant periods for which the SnPM statistic exceeded the supra-critical threshold ($p < 0.01$) and effect size was over 0.4. Colormap represents Cohen's d effect size. CO: control, F: flexible FOs, P: flexible FOs with posting, R: rigid FOs.

Fig. 3 - Foot joint moments during the stance phase. Top graph shows the mean foot joint moment of each condition with 95% confidence interval cloud (control condition). In the bottom graph, bars indicate significant periods for which the SnPM {t} statistic exceeded the supra-critical threshold ($p < 0.01$). Colormap represents Cohen's d effect size. CO: control, F: flexible FOs, P: flexible FOs with posting, R: rigid FOs.

Fig. 4 - Knee abduction moments during the stance phase. Top graph shows the mean knee abduction moment of each condition with 95% confidence interval cloud (control condition). In the bottom graph, bars indicate significant periods for which the SnPM {t} statistic exceeded the supra-critical threshold ($p < 0.01$). Colormap represents Cohen's d effect size. CO: control, F: flexible FOs, P: flexible FOs with posting, R: rigid FOs.

Figures

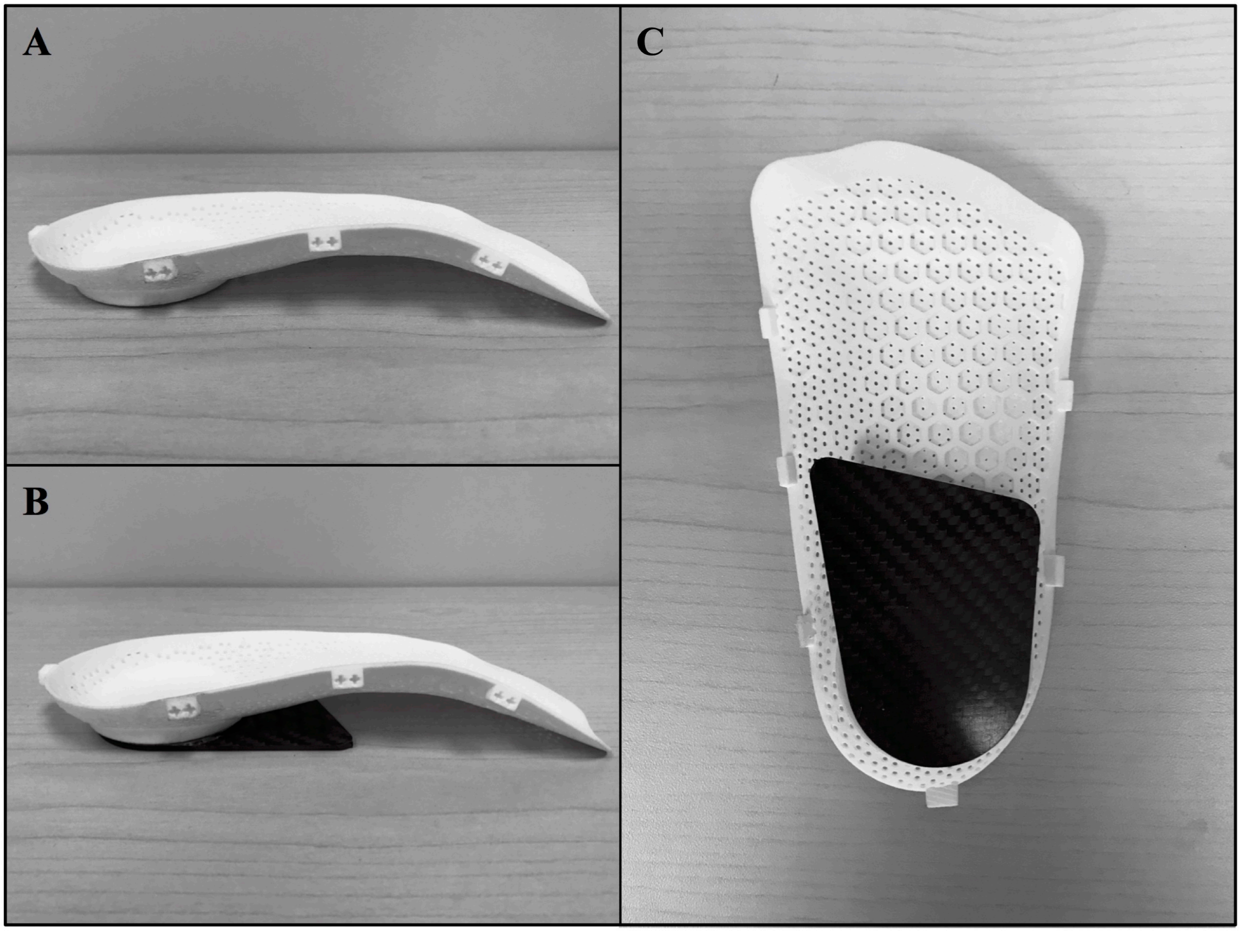

Fig. 1

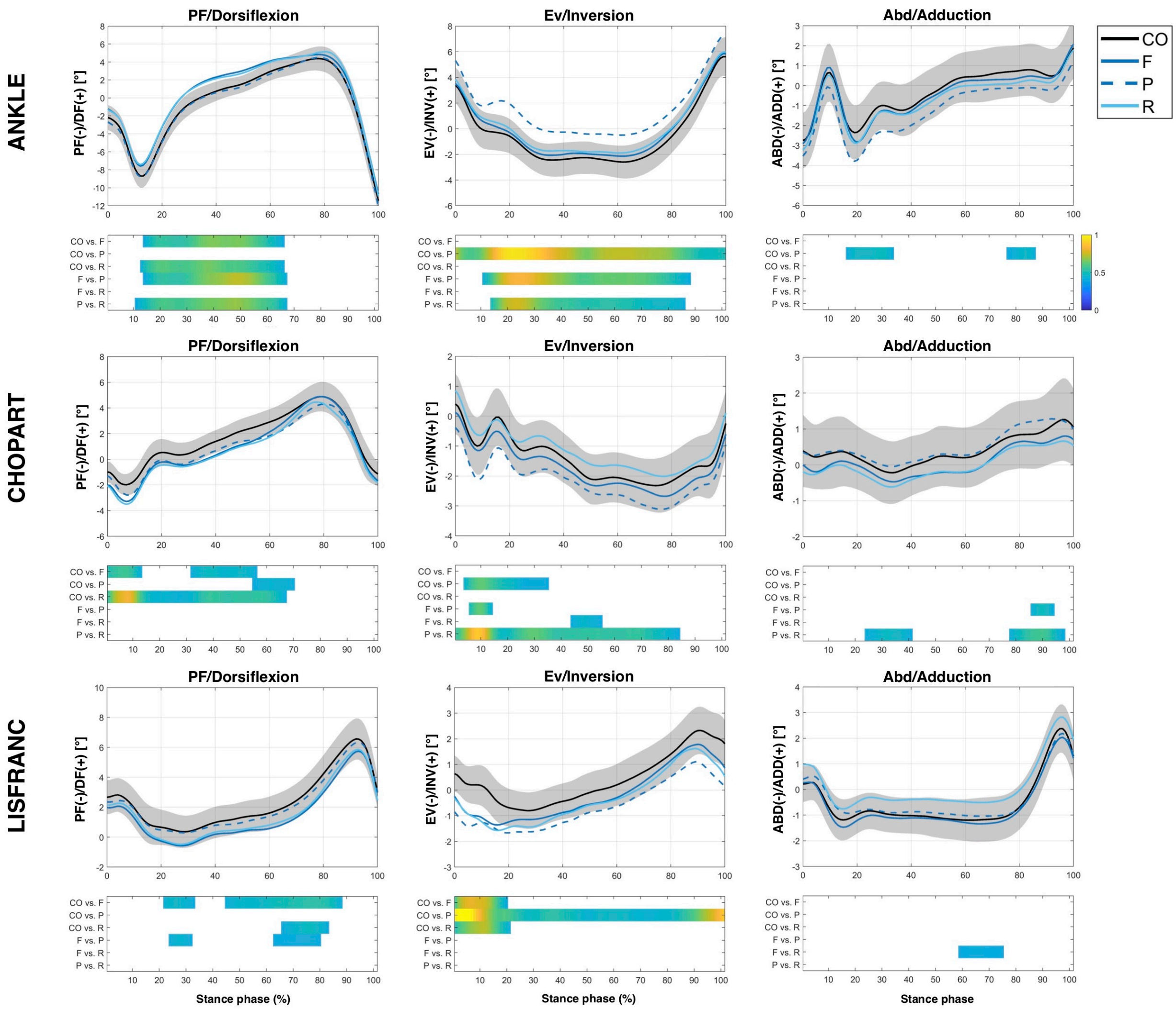
ANKLE
CHOPART
LISFRANC
PF/Dorsiflexion
Ev/Inversion
Abd/Adduction
PF(-)/DF(+) [°]
EV(-)/INV(+) [°]
ABD(-)/ADD(+) [°]
CO
F
P
R
CO vs. F
CO vs. P
CO vs. R
F vs. P
F vs. R
P vs. R
Stance phase (%)
Stance phase (%)
Stance phase

Fig. 2

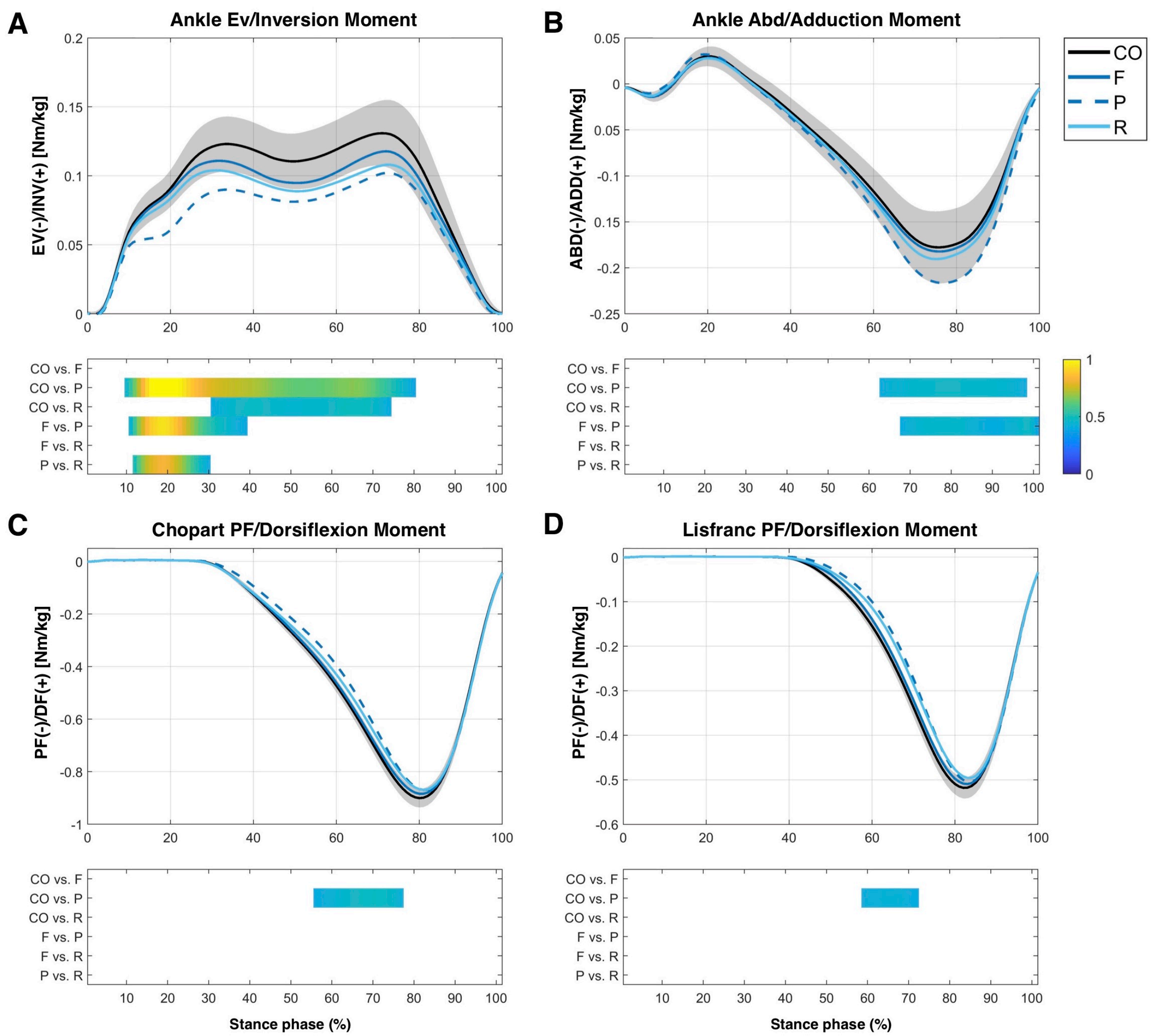
A
Ankle Ev/Inversion Moment
EV(-)/INV(+) [Nm/kg]
B
Ankle Abd/Adduction Moment
ABD(-)/ADD(+) [Nm/kg]
CO
F
P
R
C
Chopart PF/Dorsiflexion Moment
PF(-)/DF(+) [Nm/kg]
D
Lisfranc PF/Dorsiflexion Moment
PF(-)/DF(+) [Nm/kg]
CO vs. F
CO vs. P
CO vs. R
F vs. P
F vs. R
P vs. R
Stance phase (%)

481

482 **Fig. 3**

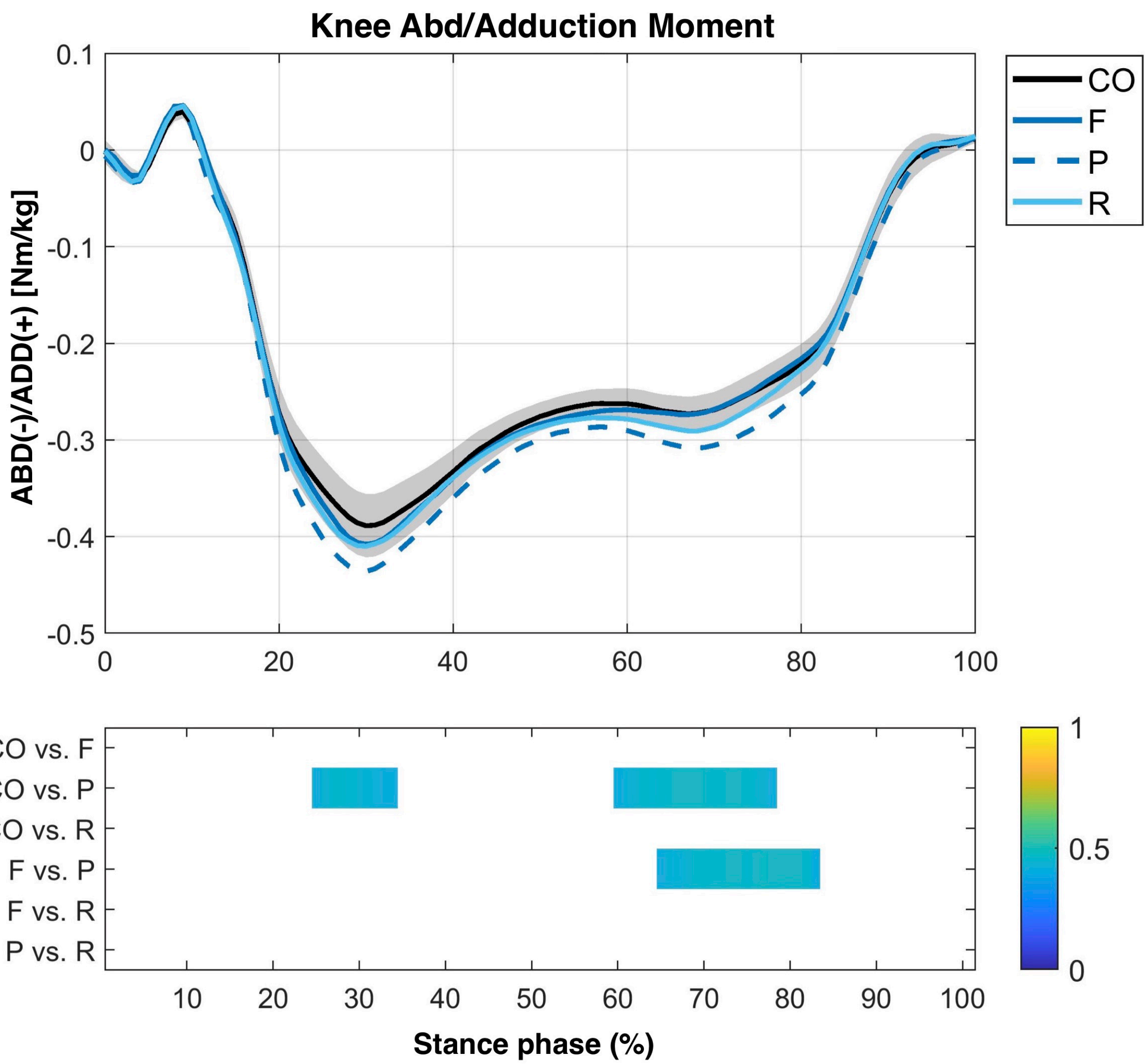

Knee Abd/Adduction Moment
ABD(-)/ADD(+) [Nm/kg]
0.1
0
-0.1
-0.2
-0.3
-0.4
-0.5
0
20
40
60
80
100
CO
F
P
R
CO vs. F
CO vs. P
CO vs. R
F vs. P
F vs. R
P vs. R
10
20
30
40
50
60
70
80
90
100
1
0.5
0
Stance phase (%)

483

484 **Fig. 4**

Table 1 - Summary of kinematic significant results

Outcome	Conditions	*Cluster range (%stance)*	*Mean difference (°)*	Mean effect size
Ankle				
PF(-)/DF(+)	Control vs. Flex	13 – 65	-1.4	0.57
	Control vs. Rigid	12 – 65	-1.3	0.57
	Flex vs. Posting	13 – 66	1.6	0.60
	Posting vs. Rigid	10 – 66	1.5	0.59
EV(-)/INV(+)	Control vs. Posting	0 – 100	-2.0	0.71
	Flex vs. Posting	9 – 87	-1.7	0.64
	Posting vs. Rigid	12 – 85	1.5	0.56
ABD(-)/ADD(+)	Control vs. Posting	16 – 33 / 76 – 86	1.3 / 0.9	0.46 / 0.44
Chopart				
PF(-)/DF(+)	Control vs. Flex	0 – 12 / 31 – 55	1.2 / 1.0	0.53 / 0.45
	Control vs. Posting	54 – 69	1.0	0.43
	Control vs. Rigid	0 – 66	1.1	0.54
EV(-)/INV(+)	Control vs. Posting	2 – 34	0.9	0.49
	Flex vs. Posting	4 – 13	0.9	0.54
	Flex vs. Rigid	42 – 54	-0.7	0.43
	Posting vs. Rigid	0 – 83	-1.1	0.57
ABD(-)/ADD(+)	Flex vs. Posting	84 – 93	-0.6	0.45
	Posting vs. Rigid	22 – 40 / 76 – 97	0.5 / 0.6	0.54 / 0.64
Lisfranc				
PF(-)/DF(+)	Control vs. Flex	20 – 32 / 43 – 87	0.9 / 1.1	0.44 / 0.48
	Control vs. Rigid	64 – 82	1.0	0.45
	Flex vs. Posting	22 – 31 / 61 – 79	-0.9 / -0.9	0.43 / 0.41
EV(-)/INV(+)	Control vs. Flex	0 – 19	1.1	0.68
	Control vs. Posting	0 – 100	1.0	0.58
	Control vs. Rigid	0 – 20	1.1	0.62
ABD(-)/ADD(+)	Flex vs. Rigid	58 – 74	-0.8	0.41

PF: Plantarflexion, DF: Dorsiflexion, EV: Eversion, INV: Inversion, ABD: Abduction, ADD: Adduction, MLA: Medial longitudinal arch, ER: External Rotation, IR: Internal Rotation.

Table 2 - Summary of joint moments significant results

Outcome	**Conditions**	***Cluster range (%stance)***	***Mean difference (Nm/kg)***	**Mean effect size**
Ankle				
EV(-)/INV(+)	Control vs. Posting	8 – 78	0.029	0.71
	Control vs. Rigid	30 – 73	0.022	0.46
	Flex vs. Posting	10 – 37	0.023	0.66
	Posting vs. Rigid	11 – 29	-0.019	0.65
ABD(-)/ADD(+)	Control vs. Posting	62 – 97	0.030	0.45
	Flex vs. Posting	67 – 99	0.025	0.44
Chopart				
PF(-)/DF(+)	Control vs. Posting	55 – 76	-0.074	0.45
Lisfranc				
PF(-)/DF(+)	Control vs. Posting	57 – 71	-0.061	0.42
Knee				
ABD(-)/ADD(+)	Control vs. Posting	24 – 33 / 59 – 77	0.047 / 0.035	0.43 / 0.45
	Flex vs. Posting	64 – 82	0.036	0.45

PF: Plantarflexion, DF: Dorsiflexion, EV: Eversion, INV: Inversion, ABD: Abduction, ADD: Adduction, MLA: Medial longitudinal arch, ER: External Rotation, IR: Internal Rotation.

Supplementary Materials

Table S1. Anatomical landmarks (Labels)

Label	**Description**	**Related segment**
LASIS	Anterior Superior Iliac Spine	Pelvis
RASIS		
LPSIS	Posterior Superior Iliac Spine	
RPSIS		
TC	Greater Trochanter	Thigh
TA	Thigh Anterior	
TP	Thigh Posterior Cluster	
TD	Thigh Down	
LC	Lateral femur Condyle	
MC	Medial femur Condyle	
HF	Head of Fibula	Shank
TT	Tibial Tuberosity	
SLU	Shank Lateral Up	
SMU	Shank Medial Up	
SMM	Shank Medial Mid Cluster	
SML	Shank Medial Low	
SLL	Shank Lateral Low	
LM	Lateral Malleolus	
MM	Medial Malleolus	
CA	Calcaneus	Rearfoot
PT	Peroneal Tubercule	
ST	Sustentaculum Tali	
TN	Navicular Tuberosity	Midfoot
CUB	Cuboid (2/3 of the distance between PT and VMB)	
ID	Midpoint between TN and CUB	
VMB	Fifth Metatarsal Base	Forefoot
SMB	Second Metatarsal Base	
FMB	First Metatarsal Base	
VMH	Fifth Metatarsal Head	
SMH	Second Metatarsal Head	
FMH	First Metatarsal Head	
PM	Proximal Phalanx of the Hallux	Hallux

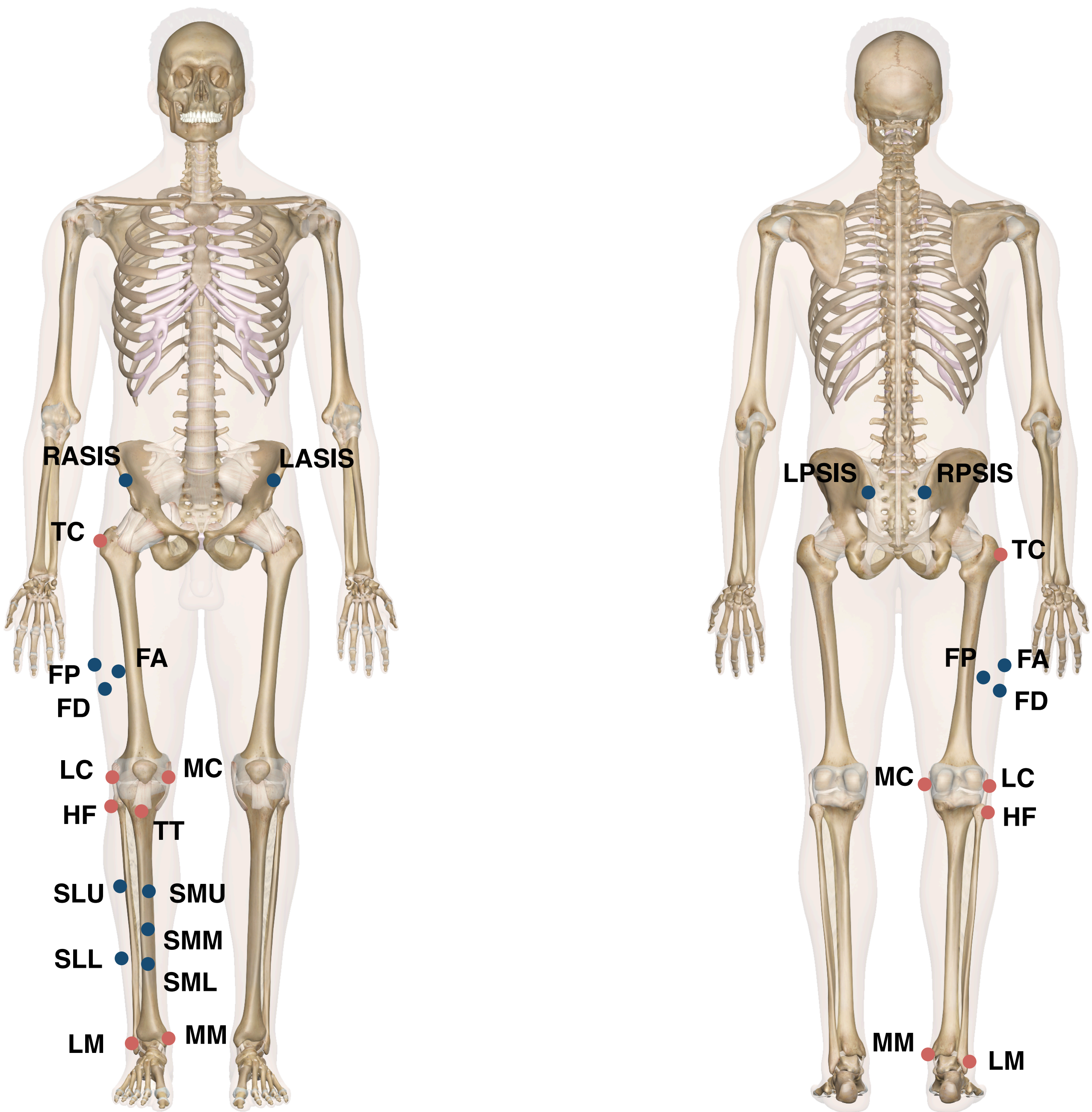

Fig. S1 - Lower-limb anatomical landmarks

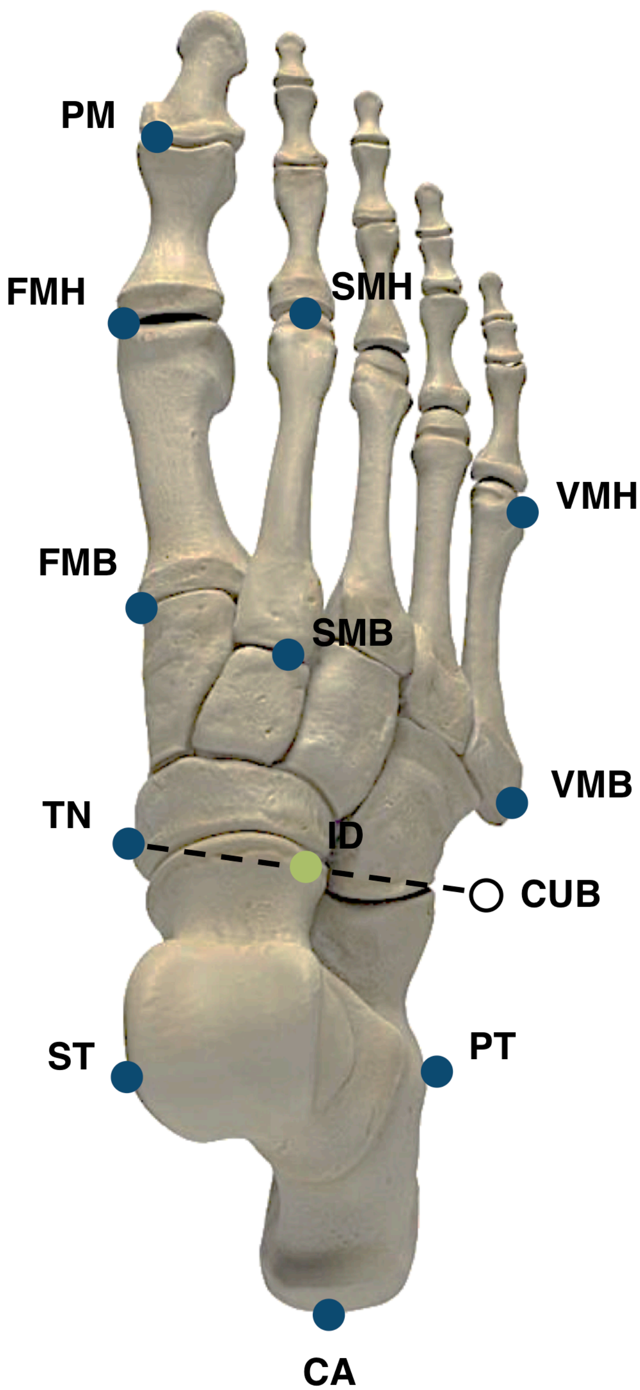

Fig. S2 - Foot anatomical landmarks

Fig. S3 – Marker set used for motion analysis

Table S2. FOs thickness and deformation during walking

	Right FO honeycomb height at medial arch (mm)		Right FO average maximum downward deformation during walking (mm)	
Subject	**Flexible**	**Rigid**	**Flexible**	**Rigid**
1	1.75	2.5	6.0	4.4
2	2.75	5	12.2	12.2
3	3	5.25	7.8	3.8
4	1.75	2.25	3.5	4.4
5	2	3.75	11.5	5.0
6	1.75	2.75	5.3	3.7
7	1.75	3	7.5	6.4
8	2.5	4.5	6.0	4.6
9	1.75	3.5	8.2	5.6
10	1.75	2.75	11.2	6.4
11	1.75	2.75	6.6	9.1
12	1.75	3	16.5	6.1
13	1.75	2.25	4.0	4.2
14	1.75	2.5	3.6	6.5
15	3	4.5	5.6	4.3
16	2.5	2.25	4.2	6.1
17	1.75	2.5	X	X
18	1.75	3	X	X
19	1.75	3.25	6.8	6.0
Mean	**2.03**	**3.22**	**7.5**	**5.8**
Std	0.45	0.92	3.5	2.1